

An aphrodisiac produced by *Vibrio fischeri* stimulates mating in the closest living relatives of animals

Arielle Woznica^{a,1}, Joseph P Gerdt^{b,1}, Ryan E. Hulett^a, Jon Clardy^{b,2}, and Nicole King^{a,2}

^a Howard Hughes Medical Institute and Department of Molecular and Cell Biology, University of California, Berkeley, California 94720, United States

^b Department of Biological Chemistry and Molecular Pharmacology, Harvard Medical School, 240 Longwood Avenue, Boston MA 02115, United States

¹ These authors contributed equally to this work.

² Co-corresponding authors, jon_clardy@hms.harvard.edu and nking@berkeley.edu.

Abstract

We serendipitously discovered that the marine bacterium *Vibrio fischeri* induces sexual reproduction in one of the closest living relatives of animals, the choanoflagellate *Salpingoeca rosetta*. Although bacteria influence everything from nutrition and metabolism to cell biology and development in eukaryotes, bacterial regulation of eukaryotic mating was unexpected. Here we show that a single *V. fischeri* protein, the previously uncharacterized EroS, fully recapitulates the aphrodisiac activity of live *V. fischeri*. EroS is a chondroitin lyase; although its substrate, chondroitin sulfate, was previously thought to be an animal synapomorphy, we demonstrate that *S. rosetta* produces chondroitin sulfate and thus extend the ancestry of this important glycosaminoglycan to the premetazoan era. Finally, we show that *V. fischeri*, purified EroS, and other bacterial chondroitin lyases induce *S. rosetta* mating at environmentally-relevant concentrations suggesting that bacterially-produced aphrodisiacs likely regulate choanoflagellate mating in nature.

Keywords: choanoflagellate; *Vibrio*; chondroitin sulfate; chondroitinase; swarming; mating; host-microbe

1 **Introduction**

2 Bacterial–eukaryotic interactions are ubiquitous, and the influences of bacteria on
3 eukaryotes vary from subtle to profound. Yet, because eukaryotes are often associated
4 with complex and unseen communities of bacteria, the breadth of eukaryotic biological
5 processes regulated by bacteria and the underlying molecular dialogue often remain
6 obscure. Nonetheless, studies of experimentally tractable host-microbe pairs have
7 revealed a growing number of examples in which bacteria regulate eukaryotic cell
8 biology and development, in some cases using molecular cues that mediate
9 pathogenesis in other contexts (Koropatnick et al., 2004).

10 One of the closest living relatives of animals, the marine choanoflagellate *S.*
11 *rosetta*, has emerged as an attractive model for uncovering bacterial cues that regulate
12 eukaryotic development. Like all choanoflagellates, *S. rosetta* survives by eating
13 bacteria (Dayel and King, 2014; Leadbeater, 2015). However, interactions between *S.*
14 *rosetta* and bacteria extend far beyond those of predator and prey. In prior work, we
15 demonstrated that the developmental switch triggering the formation of multicellular
16 “rosettes” from a single founding cell (Fairclough et al., 2010) is regulated by specific
17 lipids produced by the environmental bacterium *Algoriphagus machipongonensis*
18 (Alegado et al., 2012; Cantley et al., 2016; Woznica et al., 2016). Rosette development
19 is one of at least six different developmental switches in the sexual and asexual phases
20 of *S. rosetta*’s dynamic life history (Dayel et al., 2011; Levin and King, 2013), but until
21 now was the only choanoflagellate process known to be regulated by bacterial cues.

22 We report here on our serendipitous discovery that sexual reproduction in *S.*
23 *rosetta* is regulated by a secreted cue from the marine bacterium *Vibrio fischeri*.

24 **Results**

25 ***S. rosetta* forms mating swarms upon exposure to *V. fischeri***

26 *V. fischeri* is perhaps best understood as a model for bacterial quorum sensing
27 and as a symbiont required for the induction of light organ development in the squid,
28 *Euprymna scolopes* (Mcfall-Ngai, 2014). Although *Vibrio* spp. are known symbionts,
29 commensals, and pathogens of animals (Thompson et al., 2006), *V. fischeri* does not
30 induce rosette development (Alegado et al., 2012) and was not previously known to
31 influence any aspect of *S. rosetta* biology. We were therefore surprised to observe that
32 the addition of live *V. fischeri* bacteria to a culture of single-celled, motile *S. rosetta*
33 induced cells to gather rapidly into loose aggregates or “swarms,” each composed of
34 between 2-50 cells (Figures 1A,B, Figure S1A, Supplemental Movie 1). This dynamic
35 and previously unobserved swarming behavior began as early as 15 minutes after
36 induction with *V. fischeri*, with individual *S. rosetta* cells often moving between swarms
37 that periodically broke apart or merged with other swarms. In its timescale, mechanism,
38 and outcome, swarming was clearly unrelated to the *Algoriphagus*-induced
39 developmental process by which a single *S. rosetta* cell divides repeatedly to form a
40 rosette (Fairclough et al., 2010).

41 Although swarming has not previously been reported in choanoflagellates and
42 the biological significance of swarming in *S. rosetta* was not immediately obvious,
43 swarming is associated with mating in diverse motile eukaryotes, including amoebae,
44 ciliates, crustaceans, insects, fish, birds, and bats (Avery, 1984; Buskey, 1998; Downes,
45 1969; Giese, 1959; O'Day, 1979; Veith et al., 2004; Watson et al., 2003). Therefore, we
46 hypothesized that swarming in *S. rosetta* might indicate mating. To investigate whether

47 *V. fischeri*-induced swarming is a prelude to mating, we sought to determine whether
48 the hallmarks of mating in microbial eukaryotes (cell fusion, nuclear fusion, and meiotic
49 recombination (Bell, 1988; Dini and Nyberg, 1993; Levin and King, 2013)) occur in *S.*
50 *rosetta* following treatment with *V. fischeri*.

51 Our lab previously found that starved *S. rosetta* cells mate at low frequencies
52 (<2% of the population) after starvation for 11 days (Levin and King, 2013; Levin et al.,
53 2014). In contrast, as early as 30 minutes after induction with live *V. fischeri* or
54 conditioned medium isolated from a *V. fischeri* culture, *S. rosetta* cells formed swarms
55 and then began to pair up and fuse (Figure 1C and Supplemental Movie 2). Once paired,
56 cell fusion took as little as three minutes and all observed cell pairs were oriented with
57 their basal poles (opposite the flagellum) touching. Paired cells subsequently fused
58 along the basal pole, resulting in the formation of a binucleate cell harboring two flagella
59 (Figure 1D). After cell fusion, the two nuclei congressed and fused, and one of the two
60 parental flagella eventually retracted (Figure S1B), resulting in a diploid cell.

61 While cell fusion and nuclear fusion are consistent with mating, parasexual
62 processes can occur in the absence of meiotic recombination (Goodenough and
63 Heitman, 2014). Therefore, to test whether swarming was associated with the initiation
64 of a true sexual cycle, we used *V. fischeri* to induce the formation of heterozygous
65 diploids in *S. rosetta* cultures and then examined their offspring for evidence of meiosis
66 and recombination (Figure 1E). To produce heterozygous diploid cells, two haploid *S.*
67 *rosetta* strains (R+ and R-) containing previously characterized polymorphisms (Levin
68 et al., 2014) were mixed either in the presence of *V. fischeri* conditioned medium
69 (VFCM), or in conditioned medium from *Echinicola pacifica* (EPCM), a prey bacterium

70 (Levin et al., 2014) that does not induce swarming, as a negative control (Figure 1E).
71 After VFCM or EPCM exposure, 48 clones were isolated from each culture condition.
72 Although we cannot directly measure the ploidy of live *S. rosetta* cells, heterozygous
73 diploids can be readily identified by genotyping. While all clones (48/48) reared from the
74 EPCM-treated culture contained un-recombined parental genotypes, 10/48 clones
75 isolated following VFCM treatment were shown by genotyping to be heterozygous
76 diploids. We surmised that the heterozygous diploids were the result of outcrossed
77 mating, and found that further passaging of these clones yielded motile haploid progeny.
78 147 haploid progeny from three different heterozygous diploids were clonally isolated
79 and genotyped at polymorphic sites across the genome, providing evidence for
80 independent assortment and meiotic recombination (Figure 1E and Supplemental File
81 1). Taken together, these results demonstrate that *V. fischeri* produces an aphrodisiac
82 that induces swarming and mating in *S. rosetta*.

83

84 **Bioactivity-guided fractionation revealed that the *V. fischeri* aphrodisiac is a
85 protein**

86 Automated image analysis of *S. rosetta* cells swarming in response to VFCM
87 provided the basis for a quantitative bioassay of mating induction (Figure 2A,B and
88 Methods). As a baseline, we found that 30 minutes after treatment with VFCM, *S.*
89 *rosetta* cells consistently formed swarms containing between 5-35 cells each, whereas
90 cells did not form clusters in response to EPCM. Using this bioassay, we first tested
91 whether *V. fischeri* cues involved in quorum sensing (e.g. homoserine lactones) (Lupp
92 and Ruby, 2005; Lupp et al., 2003) or those required for its symbiosis with the squid

93 *Euprymna scolopes* (e.g. lipopolysaccharide (LPS) and peptidoglycan (PGN))
94 (Koropatnick et al., 2004; Shibata et al., 2012) might contribute to swarming induction in
95 *S. rosetta*. A set of five different *V. fischeri* mutant strains that are deficient in quorum
96 sensing were all wild type for swarming induction (Lupp and Ruby, 2005; Lupp et al.,
97 2003), as were seven mutants in polysaccharide export pathways required for
98 symbiosis with *E. scolopes* (Shibata et al., 2012) (Supplemental Table 1). Moreover,
99 treatment of *S. rosetta* with purified quorum sensing molecules (Supplemental Table 2)
100 and *V. fischeri* outer membrane vesicles (OMVs) containing LPS and PGN
101 (Beemelmanns et al., 2014) (Figure S2A) also failed to elicit mating, suggesting that the
102 cue(s) required for *S. rosetta* mating induction likely differ from factors required either
103 for quorum sensing or squid colonization.

104 We next turned to an unbiased, activity-guided fractionation and found that the
105 aphrodisiac was enriched in VFCM, including after depletion of OMVs (Figure S2A). The
106 aphrodisiac produced by *V. fischeri* could be recovered from VFCM by ammonium
107 sulfate precipitation, and the activity of the ammonium sulfate fraction was sensitive to
108 both heat and protease treatment, suggesting that the activity might be proteinaceous
109 (Figure 2C). We therefore separated all proteins precipitated from VFCM by size
110 exclusion and anion exchange chromatography, and tested the protein fractions in the
111 swarming bioassay (Figure 2A-C and Figure S2B). The swarming activity tracked with a
112 single ~90kD protein, which was revealed by mass spectrometry to be the
113 uncharacterized *V. fischeri* protein VF_A0994, hereafter referred to as EroS for
114 Extracellular regulator of Sex (Figure 2C and Supplemental File 2; GenPept Accession
115 YP_206952). To test whether EroS was sufficient to induce swarming in *S. rosetta*, we

116 heterologously expressed the *eroS* gene in *E. coli* and found that the purified protein
117 recapitulated the swarm-inducing activity of live *V. fischeri* and VFCM (Figure 2D).
118 Purified EroS protein was also sufficient to induce mating between two *S. rosetta* strains
119 (R+ and R-; Supplemental Table 3), demonstrating that a single protein secreted by *V.*
120 *fischeri* is sufficient to induce both swarming and mating in *S. rosetta*.

121

122 **EroS protein is a chondroitinase**

123 To understand the mechanism by which *V. fischeri* induces choanoflagellate
124 mating, we set out to determine the biochemical function of EroS. The EroS protein
125 sequence contains a predicted glycosaminoglycan (GAG) lyase domain (supported by
126 the detection of PFAM domains PF08124, PF02278, PF02884; (Finn et al., 2016)).
127 GAGs are linear polysaccharides that are integral components of the animal
128 extracellular matrix (ECM). GAG lyases depolymerize GAGs through an elimination
129 mechanism that distinguishes them from hydrolases, and are produced by a subset of
130 primarily pathogenic bacteria and fungi (Zhang et al., 2010), as well as by human
131 commensals, including gut bacteria in the genus *Bacteroides* (Ahn et al., 2011; Hong et
132 al., 2002). Through the alignment of the EroS protein sequence with multiple bacterial
133 GAG lyases with solved structures, we found that EroS harbors conserved residues at
134 sites required for catalytic activity (His-278 and Tyr-287; Figure 3A) (Han et al., 2014;
135 Linhardt et al., 2006; Shaya et al., 2008; Weijun Huang et al., 2001).

136 Sulfated GAGs are thought to be eumetazoan-specific innovations (DeAngelis,
137 2002a; Yamada et al., 2011), and are not known to exist in choanoflagellates. (Although
138 some pathogenic bacteria evade host immune responses by producing extracellular

139 GAGs, these molecules are produced by way of an independently evolved biosynthetic
140 pathway and, unlike animal GAGs, are not modified by sulfation (DeAngelis, 2002b)).
141 Moreover, GAGs are diverse and the substrate specificities of GAG lyases cannot be
142 deduced from sequence alone (Zhang et al., 2010). Therefore, we next set out to
143 answer three questions: (1) does EroS exhibit GAG-degrading activity, (2) is the
144 enzymatic activity of EroS required for its function as an aphrodisiac, and (3) what are
145 its substrates in *S. rosetta*?

146 We found that purified EroS protein degrades GAG substrates *in vitro*, and is
147 thus a *bona fide* GAG lyase. GAGs are classified based on their disaccharide units:
148 heparan sulfate, chondroitin sulfate, dermatan sulfate, hyaluronic acid, and keratan
149 sulfate (Zhang et al., 2010). EroS showed strong lyase activity toward purified
150 chondroitin sulfate and hyaluronan, but not heparan sulfate or dermatan sulfate (Figure
151 3B and Figure S2C,D). We did not test keratan sulfate because it does not contain
152 uronic acid and therefore cannot be degraded by GAG lyases (Garron and Cygler,
153 2010).

154 We next asked whether the enzymatic activity of EroS is important to its function
155 as an aphrodisiac. Alanine substitution at conserved catalytic residues (His-278 and
156 Tyr-287) required for chondroitin and hyaluronan degradation in other chondroitin lyases
157 eliminated the ability of EroS to induce swarming in *S. rosetta* (Fig. 3C) (Linhardt et al.,
158 2006). Moreover, well-characterized chondroitin lyases from other bacteria (ABC
159 chondroitinase from *Proteus vulgaris* and AC chondroitinase from *Flavobacterium*
160 *heparinum*) induced swarming and mating in *S. rosetta* at levels resembling those
161 induced by EroS (Figure 3C and Supplemental Table 3), indicating that the

162 chondroitinase activity of EroS is both necessary and sufficient for its function as an
163 aphrodisiac.

164 Although sulfated GAGs were previously thought to be restricted to animals, key
165 heparan biosynthetic enzymes have been detected in the genome of the
166 choanoflagellate *Monosiga brevicollis* (Ori et al., 2011), and we have further found that
167 the *S. rosetta* genome encodes homologs of enzymes required for chondroitin
168 biosynthesis (Figure 4A, Figure S3A, Supplemental File 3) (Fairclough et al., 2013; King
169 et al., 2008). To test whether chondroitin is produced by *S. rosetta*, we treated
170 polysaccharides isolated from motile *S. rosetta* cells with the broad specificity ABC
171 chondroitinase from *P. vulgaris*. The *P. vulgaris* ABC chondroitinase liberated
172 chondroitin disaccharides, demonstrating that *S. rosetta* indeed produces chondroitin
173 (Figure 4B, Figure S3B,C). Finally, to test whether EroS can degrade *S. rosetta*
174 chondroitin we treated *S. rosetta* polysaccharides with EroS and found that it released
175 unsulfated chondroitin and chondroitin-6-sulfate disaccharides, indicating that *S. rosetta*
176 chondroitin is a target of EroS (Figure 4B, Figure S3B,C).

177 Chondroitin sulfate in animal ECM can be found covalently linked to core proteins,
178 thus forming proteoglycans. To determine whether chondroitin disaccharides released
179 from proteoglycans play a role in stimulating mating, we tested various products of EroS
180 digestion for aphrodisiac activity (Figure S4). Conditioned media from EroS-treated *S.*
181 *rosetta* cells did not trigger swarming in naïve *S. rosetta*, nor did the digested products
182 of commercial chondroitin sulfate treated with EroS. Moreover, swarming was not
183 induced by any combination or concentration of unsulfated and 6-sulfated chondroitin
184 disaccharides tested (Figure S4). These results lead us to hypothesize that the

185 structural modification of *S. rosetta* proteoglycans by EroS, rather than the chondroitin
186 disaccharide products of EroS digestion, are important for activating the swarming and
187 mating pathway in *S. rosetta*.

188 Finally, because swarming has not been previously described in
189 choanoflagellates, we investigated whether *V. fischeri* might induce swarming under
190 plausible environmental conditions. We found that EroS is secreted constitutively by *V.*
191 *fischeri* when grown under either high or low nutrient conditions (Supplemental Table 4).
192 Cultures of *S. rosetta* swarm in response to as little as 4×10^2 *V. fischeri* cells/mL – a
193 density comparable to that of *V. fischeri* in oligotrophic oceans (from 6×10^2 cells/mL to
194 $> 1 \times 10^4$ cells/mL during blooms (Jones et al., 2007)) – within 30 minutes of exposure
195 (Figure S5). Moreover, EroS was sufficient to trigger robust swarming in *S. rosetta* at
196 concentrations as low as 5 pM (Figure S5), making EroS as potent as the sex
197 pheromones produced by volvocine algae (Kochert, 2012) and by marine invertebrates
198 (Bartels-Hardege et al., 1996; Li et al., 2002). Together, these data suggest that *V.*
199 *fischeri* or other chondroitinase-producing bacteria could plausibly trigger *S. rosetta*
200 swarming and mating *in natura*.

201

202 **Discussion**

203 We have discovered that a secreted bacterial chondroitinase, EroS, induces
204 mating in *S. rosetta*, one of the closest living relatives of animals. Through the study of
205 this unexpected interkingdom interaction, we found that mating in *S. rosetta* is initiated
206 in response to the degradation of chondroitin sulfate, a glycosaminoglycan previously
207 thought to be restricted to animals.

208 The first hint that *V. fischeri* might induce mating came from the observation of *S.*
209 *rosetta* swarms following exposure to the bacterium. By increasing local population
210 density, swarming has previously been found to facilitate mating in diverse amoebae,
211 flagellates, crustaceans, cnidarians, polychaetes, insects, fish, and birds (Avery, 1984;
212 Buskey, 1998; Downes, 1969; Giese, 1959; Hamner and Dawson, 2009; Omori and
213 Hamner, 1982; Sorensen and Wisenden, 2015; Watson et al., 2003). As in other
214 organisms that swarm, the connection of swarming to mating may be critical, since their
215 aquatic, pelagic lifestyle can make it challenging to find mates. Indeed, under the
216 starvation conditions that trigger *S. rosetta* mating in the absence of swarming, mating
217 takes >500X longer (~11 days) and occurs in a small fraction of the population (Levin et
218 al., 2014).

219 Most previously characterized examples of coordinated mating behaviors are
220 regulated by pheromonal cues. Conspecific swarming is initiated by diverse aggregation
221 pheromones (for example, ester and isoprenoid pheromones in beetles (Kartika et al.,
222 2015; Wertheim et al., 2005) and peptide pheromones in sea slugs (Painter et al., 2016)
223 and polychaetes (Ram et al., 1999)), and free-spawning marine animals produce
224 pheromones to synchronize gamete release and enhance fertilization success (Babcock
225 et al., 2011). Biotic and abiotic cues from the environment can also help coordinate
226 mating behavior in animals. For example, spawning in marine invertebrates is correlated
227 with phytoplankton blooms, and some sea urchins, mussels, and polychaetes spawn
228 after exposure to small molecules produced by environmental phytoplankton (Smith and
229 Strehlow, 1983; Starr et al., 1990; 1992), although these cues remain structurally
230 elusive. Just as phytoplankton blooms are hypothesized to signify a nutrient-rich

231 environment for spawning, the presence of chondroitinase-producing bacteria may
232 indicate an environmental condition, or the convergence of multiple environmental
233 factors, that favor mating in *S. rosetta*. Although *V. fischeri* was the first bacterium
234 observed to regulate mating in *S. rosetta*, we have since identified other bacteria that
235 similarly induce swarming and mating (Supplemental Table 1). Therefore, we predict
236 that mating in *S. rosetta* might be regulated by diverse species of bacteria in nature, and
237 hypothesize that swarming is a common occurrence within the natural life history of *S.*
238 *rosetta*.

239 Our discovery that *V. fischeri* produces a chondroitinase that functions as an
240 aphrodisiac also revealed that *S. rosetta* produces chondroitin sulfate, providing the first
241 biochemical evidence for this important GAG in a non-animal and extending its
242 evolutionary history to the premetazoan era. In an interesting parallel to the induction of
243 *S. rosetta* mating by a chondroitinase, GAGs and sulfated polysaccharides mediate
244 mating in diverse internally and externally fertilizing animals where they provide a
245 protective and species-specific coating around oocytes (Miller and Ax, 1990). In the
246 case of the mammalian oocyte, which is surrounded by the GAG hyaluronan, sperm
247 secrete hyaluronidase to penetrate the hyaluronan-containing coating, whereas in sea
248 urchins, sulfated polysaccharides coating the sea urchin oocyte ensure species-
249 restricted sperm activation and binding (Mengerink and Vacquier, 2001). Of course,
250 GAGs like hyaluronan and chondroitin sulfate are also essential components of the
251 ECM in somatic cells of animals, where they contribute to a range of functions that
252 include the maintenance of cell adhesion through interactions with ECM molecules, the
253 integration of signals from the extracellular milieu, and the stabilization of collagen fibers.

254 Future investigations may reveal whether chondroitin sulfate in *S. rosetta* functions to
255 mediate species-specific cell recognition in the context of fertilization and may provide
256 insight into the premetazoan roles of this important molecule. Moreover, it will be
257 fascinating to explore whether bacteria influence mating in other aquatic organisms, for
258 whom the triggers of mating are often obscure.

259

260

261

262

263

264

265

266

267

268

269

270

271

272

273

274

275

276

277

278 **Acknowledgements**

279 We thank K. Visick for *V. fischeri* *syp* deletion mutants, N. Ruby for *V. fischeri* quorum
280 sensing deletion mutants, and Y. Boucher for diverse species of *Vibrio* bacteria. We
281 thank M. Abedin, D. Booth and B. Larson for helpful discussions and critical reading of
282 the manuscript. This work used the Vincent J. Coates Proteomics/Mass Spectrometry
283 Laboratory at UC Berkeley, supported in part by NIH S10 Instrumentation Grant
284 S10RR025622, and the Complex Carbohydrate Research Center, supported by the
285 National Institutes of Health-funded Research Resource for Integrated Glycotechnology
286 (NIH grant no. P41GM103390).

287

288 **References**

289 Ahn, M.Y., Shin, K.H., Kim, D.H., Jung, E.-A., Toida, T., Linhardt, R.J., and Kim, Y.S.
290 (2011). Characterization of a *Bacteroides* species from human intestine that degrades
291 glycosaminoglycans. *Can. J. Microbiol.* **44**, 423–429.

292 Alegado, R.A., Brown, L.W., Cao, S., Dermenjian, R.K., Zuzow, R., Fairclough, S.R.,
293 Clardy, J., and King, N. (2012). A bacterial sulfonolipid triggers multicellular
294 development in the closest living relatives of animals. *Elife* **1**, e00013.

295 Avery, M.I. (1984). Lekking in birds: choice, competition and reproductive constraints.
296 *Ibis* **126**, 177–187.

297 Babcock, R., Mundy, C., Keesing, J., and Oliver, J. (2011). Predictable and
298 unpredictable spawning events: *in situ* behavioural data from free-spawning coral reef
299 invertebrates. *Invertebrate Reproduction & Development* **22**, 213–227.

300 Bartels-Hardege, H.D., Hardege, J.D., Zeeck, E., Müller, C., Wu, B.L., and Zhu, M.Y.
301 (1996). Sex pheromones in marine polychaetes: a biologically active volatile compound
302 from the coelomic fluid of female *Nereis (Neanthes) japonica*. *Journal of Experimental
303 Marine Biology and Ecology* **201**, 275–284.

304 Beemelmanns, C., Woznica, A., Alegado, R.A., Cantley, A.M., King, N., and Clardy, J.
305 (2014). Synthesis of the rosette-inducing factor RIF-1 and analogs. *J. Am. Chem. Soc.*
306 **136**, 10210–10213.

307 Bell, G. (1988). Sex and death in protozoa: the history of an obsession (Cambridge
308 University Press).

309 Buskey, E.J. (1998). Components of mating behavior in planktonic copepods. *Journal of
310 Marine Systems* **15**, 13–21.

311 Cantley, A.M., Woznica, A., Beemelmanns, C., King, N., and Clardy, J. (2016). Isolation
312 and Synthesis of a Bacterially Produced Inhibitor of Rosette Development in
313 Choanoflagellates. *J. Am. Chem. Soc.* **138**, 4326–4329.

314 Dayel, M.J., and King, N. (2014). Prey capture and phagocytosis in the choanoflagellate
315 *Salpingoeca rosetta*. *PloS One* **9**, e95577.

316 Dayel, M.J., Alegado, R.A., Fairclough, S.R., Levin, T.C., Nichols, S.A., McDonald, K.,
317 and King, N. (2011). Cell differentiation and morphogenesis in the colony-forming
318 choanoflagellate *Salpingoeca rosetta*. *Developmental Biology* **357**, 73–82.

319 DeAngelis, P.L. (2002a). Evolution of glycosaminoglycans and their
320 glycosyltransferases: implications for the extracellular matrices of animals and the
321 capsules of pathogenic bacteria. *Anat Rec* **268**, 317–326.

322 DeAngelis, P.L. (2002b). Microbial glycosaminoglycan glycosyltransferases.

323 Glycobiology 12, 9R–16R.

324 Dini, F., and Nyberg, D. (1993). Sex in Ciliates. In Advances in Microbial Ecology,
325 (Boston, MA: Springer US), pp. 85–153.

326 Downes, J.A. (1969). The swarming and mating flight of Diptera. Annual Review of
327 Entomology 14, 271–298.

328 Fairclough, S.R., Chen, Z., Kramer, E., Zeng, Q., Young, S., Robertson, H.M., Begovic,
329 E., Richter, D.J., Russ, C., Westbrook, M.J., et al. (2013). Premetazoan genome
330 evolution and the regulation of cell differentiation in the choanoflagellate *Salpingoeca*
331 *rosetta*. Genome Biol. 14, R15.

332 Fairclough, S.R., Dayel, M.J., and King, N. (2010). Multicellular development in a
333 choanoflagellate. Curr Biol 20, R875–R876.

334 Finn, R.D., Coggill, P., Eberhardt, R.Y., Eddy, S.R., Mistry, J., Mitchell, A.L., Potter, S.C.,
335 Punta, M., Qureshi, M., Sangrador-Vegas, A., et al. (2016). The Pfam protein families
336 database: towards a more sustainable future. Nucleic Acids Res 44, D279–D285.

337 Garron, M.-L., and Cygler, M. (2010). Structural and mechanistic classification of uronic
338 acid-containing polysaccharide lyases. Glycobiology 20, 1547–1573.

339 Gerber, S.A., Rush, J., Stemman, O., Kirschner, M.W., and Gygi, S.P. (2003). Absolute
340 quantification of proteins and phosphoproteins from cell lysates by tandem MS.
341 Proceedings of the National Academy of Sciences 100, 6940–6945.

342 Giese, A.C. (1959). Comparative physiology: annual reproductive cycles of marine
343 invertebrates. Annu Rev Physiol 21, 547–576.

344 Goodenough, U., and Heitman, J. (2014). Origins of eukaryotic sexual reproduction.
345 Cold Spring Harbor Perspectives in Biology 6, a016154–a016154.

346 Hager, D.A., and Burgess, R.R. (1980). Elution of proteins from sodium dodecyl sulfate-
347 polyacrylamide gels, removal of sodium dodecyl sulfate, and renaturation of enzymatic
348 activity: Results with sigma subunit of Escherichia coli RNA polymerase, wheat germ
349 DNA topoisomerase, and other enzymes. Anal. Biochem. 109, 76–86.

350 Hamner, W.M., and Dawson, M.N. (2009). A review and synthesis on the systematics
351 and evolution of jellyfish blooms: advantageous aggregations and adaptive
352 assemblages. Hydrobiologia 616, 161–191.

353 Han, W., Wang, W., Zhao, M., Sugahara, K., and Li, F. (2014). A novel eliminase from a
354 marine bacterium that degrades hyaluronan and chondroitin sulfate. J Biol Chem 289,
355 27886–27898.

356 Hong, S.W., Kim, B.T., Shin, H.Y., Kim, W.S., Lee, K.S., Kim, Y.S., and Kim, D.H.
357 (2002). Purification and characterization of novel chondroitin ABC and AC lyases from

358 Bacteroides stercoris HJ-15, a human intestinal anaerobic bacterium. The FEBS Journal
359 269, 2934–2940.

360 Jones, B.W., Maruyama, A., Ouverney, C.C., and Nishiguchi, M.K. (2007). Spatial and
361 Temporal Distribution of the Vibrionaceae in Coastal Waters of Hawaii, Australia, and
362 France. *Microb Ecol* 54, 314–323.

363 Kartika, T., Shimizu, N., and Yoshimura, T. (2015). Identification of Esters as Novel
364 Aggregation Pheromone Components Produced by the Male Powder-Post Beetle,
365 *Lyctus africanus* Lesne (Coleoptera: Lyctinae). *PLoS One* 10, e0141799.

366 King, N., Westbrook, M.J., Young, S.L., Kuo, A., Abedin, M., Chapman, J., Fairclough,
367 S., Hellsten, U., Isogai, Y., Letunic, I., et al. (2008). The genome of the choanoflagellate
368 *Monosiga brevicollis* and the origin of metazoans. *Nature* 451, 783–788.

369 Kochert, G. (2012). Sexual Pheromones in Volvox Development. *Sexual Interactions in*
370 *Eukaryotic Microbes* 73–93.

371 Koropatnick, T.A., Engle, J.T., Apicella, M.A., Stabb, E.V., Goldman, W.E., and McFall-
372 Ngai, M.J. (2004). Microbial factor-mediated development in a host-bacterial mutualism.
373 *Science* 306, 1186–1188.

374 Leadbeater, B.S.C. (2015). *The Choanoflagellates: Evolution, Ecology, and Biology*
375 (Cambridge University Press).

376 Levin, T.C., and King, N. (2013). Evidence for sex and recombination in the
377 choanoflagellate *Salpingoeca rosetta*. *Current Biology* 23, 2176–2180.

378 Levin, T.C., Greaney, A.J., Wetzel, L., and King, N. (2014). The Rosetteless gene
379 controls development in the choanoflagellate *S. rosetta*. *Elife* 3.

380 Li, W., Scott, A.P., Siefkes, M.J., Yan, H., Liu, Q., Yun, S.-S., and Gage, D.A. (2002).
381 Bile acid secreted by male sea lamprey that acts as a sex pheromone. *Science* 296,
382 138–141.

383 Linhardt, R.J., Avci, F.Y., Toida, T., Kim, Y.S., and Cygler, M. (2006). CS Lyases:
384 structure, activity, and applications in analysis and the treatment of diseases. In
385 Chondroitin Sulfate: Structure, Role and Pharmacological Activity, (Elsevier), pp. 187–
386 215.

387 Lupp, C., and Ruby, E.G. (2005). *Vibrio fischeri* uses two quorum-sensing systems for
388 the regulation of early and late colonization factors. *Journal of Bacteriology* 187, 3620–
389 3629.

390 Lupp, C., Urbanowski, M., Greenberg, E.P., and Ruby, E.G. (2003). The *Vibrio fischeri*
391 quorum-sensing systems *ain* and *lux* sequentially induce luminescence gene
392 expression and are important for persistence in the squid host. *Molecular Microbiology*
393 50, 319–331.

394 Mcfall-Ngai, M. (2014). Divining the Essence of Symbiosis: Insights from the Squid-
395 Vibrio Model. *PLoS Biol* 12, e1001783.

396 Mengerink, K.J., and Vacquier, V.D. (2001). Glycobiology of sperm-egg interactions in
397 deuterostomes. *Glycobiology* 11, 37R–43R.

398 Miller, D.J., and Ax, R.L. (1990). Carbohydrates and fertilization in animals. *Mol. Reprod.*
399 *Dev.* 26, 184–198.

400 O'Day, D.H. (1979). Aggregation during sexual development in *Dictyostelium*
401 *discoideum*. *Can. J. Microbiol.* 25, 1416–1426.

402 Omori, M., and Hamner, W.M. (1982). Patchy distribution of zooplankton: Behavior,
403 population assessment and sampling problems. *Marine Biology* 72, 193–200.

404 Ori, A., Wilkinson, M.C., and Fernig, D.G. (2011). A systems biology approach for the
405 investigation of the heparin/heparan sulfate interactome. *J Biol Chem* 286, 19892–
406 19904.

407 Painter, S.D., Clough, B., Garden, R.W., Sweedler, J.V., and Nagle, G.T. (2016).
408 Characterization of Aplysia Attractin, the First Water-borne Peptide Pheromone in
409 Invertebrates. *The Biological Bulletin* 194, 120–131.

410 Ram, J.L., Müller, C.T., Beckmann, M., and Hardege, J.D. (1999). The spawning
411 pheromone cysteine-glutathione disulfide (“nereithione”) arouses a multicomponent
412 nuptial behavior and electrophysiological activity in *Nereis succinea* males. *Faseb J* 13,
413 945–952.

414 Shaya, D., Hahn, B.-S., Bjerkan, T.M., Kim, W.S., Park, N.Y., Sim, J.-S., Kim, Y.S., and
415 Cygler, M. (2008). Composite active site of chondroitin lyase ABC accepting both
416 epimers of uronic acid. *Glycobiology* 18, 270–277.

417 Shibata, S., Yip, E.S., Quirke, K.P., Ondrey, J.M., and Visick, K.L. (2012). Roles of the
418 structural symbiosis polysaccharide (syp) genes in host colonization, biofilm formation,
419 and polysaccharide biosynthesis in *Vibrio fischeri*. *Journal of Bacteriology* 194, 6736–
420 6747.

421 Smith, J.R., and Strehlow, D.R. (1983). Algal-induced spawning in the marine mussel
422 *Mytilus californianus* 4. *International Journal of Invertebrate Reproduction* 6, 129–133.

423 Sorensen, P.W., and Wisenden, B.D. (2015). *Fish Pheromones and Related Cues*
424 (John Wiley & Sons).

425 Starr, M., Himmelman, J.H., and Therriault, J.-C. (1990). Direct Coupling of Marine
426 Invertebrate Spawning with Phytoplankton Blooms. *Science* 247, 1071–1074.

427 Starr, M., Himmelman, J.H., and Therriault, J.-C. (1992).
428 Isolation and properties of a substance from the diatom *Phaeodactylum tricornutum*

429 which induces spawning in the sea urchin *Strongylocentrotus droebachiensis*. *Marine*
430 *Ecology Progress Series* 79, 275–287.

431 Thompson, F.L., Austin, B., and Swings, J. (2006). *The biology of vibrios*. (Washington
432 (D.C.): ASM Press).

433 Veith, M., Beer, N., Kiefer, A., Johannessen, J., and Seitz, A. (2004). The role of
434 swarming sites for maintaining gene flow in the brown long-eared bat. *Heredity (Edinb)*
435 93, 342–349.

436 Wang, W., Han, W., Cai, X., Zheng, X., Sugahara, K., and Li, F. (2015). Cloning and
437 characterization of a novel chondroitin sulfate/dermatan sulfate 4-O-endosulfatase from
438 a marine bacterium. *J Biol Chem* 290, 7823–7832.

439 Watson, G.J., Bentley, M.G., Gaudron, S.M., and Hardege, J.D. (2003). The role of
440 chemical signals in the spawning induction of polychaete worms and other marine
441 invertebrates. *Journal of Experimental Marine Biology and Ecology* 294, 169–187.

442 Weijun Huang, Lorena Boju, Lydia Tkalec, Hongsheng Su, Hyun-Ok Yang, Nur Sibel
443 Gunay, Robert J Linhardt, Yeong Shik Kim, Allan Matte, A., Miroslaw Cygler (2001).
444 Active site of chondroitin AC lyase revealed by the structure of enzyme–oligosaccharide
445 complexes and mutagenesis. *Biochemistry* 40, 2359–2372.

446 Wertheim, B., van Baalen, E.-J.A., Dicke, M., and Vet, L.E.M. (2005). Pheromone-
447 mediated aggregation in nonsocial arthropods: an evolutionary ecological perspective.
448 *Annual Review of Entomology* 50, 321–346.

449 Woznica, A., Cantley, A.M., Beemelmanns, C., Freinkman, E., Clardy, J., and King, N.
450 (2016). Bacterial lipids activate, synergize, and inhibit a developmental switch in
451 choanoflagellates. *Proc Natl Acad Sci USA* 113, 7894–7899.

452 Yamada, S., Sugahara, K., and Özbek, S. (2011). Evolution of glycosaminoglycans.
453 *Communicative & Integrative Biology* 4, 150–158.

454 Zhang, F., Zhang, Z., and Linhardt, R.J. (2010). Glycosaminoglycans. In *Handbook of*
455 *Glycomics*, (Elsevier), pp. 59–80.

456

457

458

459 **Methods**

460

461

462 **Culture media**

463 Artificial seawater (ASW), cereal grass media (CG media), and Sea Water

464 Complete media (SWC) were prepared as described previously (Levin and King, 2013;

465 Woznica et al., 2016). Artificial sea water (ASW) was made by adding 32.9 g Tropic

466 Marin sea salts (Wartenberg, Germany) to 1L distilled water to a salinity of 32-27 parts

467 per thousand. SWC media was made by adding 250 mg/L peptone, 150 mg/L yeast

468 extract, 150 L/L glycerol in artificial sea water. CG media was made by infusing ASW

469 with cereal grass pellets (Basic Science Supplies, Rochester NY).

470 **Choanoflagellate husbandry**

471 SrEpac (Levin and King, 2013) (*S. rosetta* grown in the presence of *Echinicola*

472 *pacifica* bacteria, ATCC PRA-390) was propagated in 5% Sea Water Complete media

473 (SWC diluted to 5% vol/vol in ASW) at 22°C. SrEpac was passaged 1:20 into 19mL

474 fresh 5% SWC every other day to obtain stationary growth phase cultures (cells were

475 grown in 25cm² Corning cell culture flask). Prior to all induction bioassays, unless

476 otherwise indicated, cells were diluted to approximately 1x10⁵ cells/mL in ASW at the

477 time of induction.

478 **Immunofluorescence microscopy**

479 Stationary-phase cells were induced with *V. fischeri* conditioned media or *E.*

480 *pacifica* conditioned media and fixed at intervals of 10 minutes, 30 minutes, 1 hour, 2

481 hours, and 4 hours after induction. After vortexing, cells were fixed for 5 min in 6%

482 acetone followed by 10 minutes in 4% formaldehyde. Cells were then allowed to settle

483 for 30 min onto poly-L-lysine coated coverslips (BD Bioscience). Cells were stained with

484 E7 anti-tubulin antibody (1:200; Developmental Studies Hybridoma Bank), Alexa Fluor
485 488 anti-mouse (1:1000; Molecular Probes), and .01mg/mL Hoechst 3342 (Thermo
486 Fischer) before mounting in Prolong Gold antifade reagent (Molecular Probes). Cells
487 were imaged at 63x using a Zeiss LSM 880 AxioExaminer with Airyscan.

488 Mating stages were assigned based on the following criteria: orientation of paired
489 cells, fusion of cell bodies, localization and number nuclei, number of flagella. Cell
490 fusion could be clearly distinguished from cell division for several reasons, including (1)
491 fusing cells are paired basally, whereas recently divided sister cells are paired laterally,
492 (2) flagella remain elongated during the fusion process, but are retracted throughout cell
493 division and (3) DNA remains uncondensed throughout cell fusion, but is condensed
494 during cell division.

495 **Isolation of conditioned media (including VFCM and EPCM)**

496 *Vibrio fischeri* ES114 (ATCC 700601) and all other *Vibrio* species (Supplemental
497 Table 2) were grown by shaking in 200mL 100% SWC media for 30H at 20°C, and
498 pelleted by centrifugation. *E. pacifica* was grown by shaking in 200mL 100% SWC for
499 30H at 30°C, and pelleted by centrifugation. Cell-free supernatant was then vacuum
500 filtered twice through a 0.22 mM filter (EMD Millipore Stericup) to obtain 100% CM.
501 Concentrated conditioned media was obtained using 30kD and 50kD molecular weight
502 cut off centrifugal filter units (Amicon).

503 **Inducing mating and meiosis**

504 *S. rosetta* strains: All crosses were performed between two *S. rosetta* strains with
505 previously verified single nucleotide polymorphisms (SNPs), R- (previously referred to
506 as Rosetteless) and R+ (previously referred to as Isolate B) (Levin et al., 2014). Prior to

507 inducing mating, stationary phase cultures were obtained by passaging Rosetteless
508 1:20 into 19mLs fresh 5% SWC media every other day, and Isolate B 1:10 into 20mLs
509 fresh 25% CG media every two days.

510 Inducing mating: Stationary phase R+ and R- cultures were counted and diluted to the
511 same cell density (1×10^6 cells/mL). R+ and R- cultures were mixed in equal proportions,
512 pelleted, and resuspended in fresh 25% CG media to obtain a final cell density of 1×10^6
513 cells/mL. Mating crosses were performed in 2mL total volumes under the following
514 induction conditions: 5% (V/V) *E. pacifica* conditioned media (EPCM), 5% (V/V) *Vibrio*
515 *fischeri* conditioned media (VFCM), 0.5nM VF_rGAG lyase, 5 “units” Chondroitinase
516 ABC (Sigma C3667), and 5 “units” Chondroitinase AC (Sigma C2780). Cells were
517 allowed to mate for 16 hours, after which the induced culture was pelleted and washed
518 twice in 25% CG media to prevent further mating prior to limiting dilution.

519 Isolating diploids by limiting dilution: Mated cells were clonally isolated by limiting
520 dilution into 96-well plates containing 25% CG media. For all crosses performed, the
521 probability of clonal isolation at this step was between 0.85 and 0.92. Although we
522 cannot directly measure the ploidy of live *S. rosetta* cells, the differentiation of
523 planktonic motile cells into substrate-attached “thecate” cells correlates with the
524 transition to diploidy (Levin et al., 2014). After five days of growth, isolates were
525 phenotyped and then divided into two populations. For each isolate, one population was
526 rapidly passaged to induce meiosis (see below), and the other population was used for
527 DNA extraction. For DNA extraction, isolates were expanded into 1mL of 5% CG media
528 to prevent meiosis, and grown for three days in 24-well plates. DNA was extracted from
529 each isolate using the following method: 500 μ L of cells were pelleted and resuspended in

530 20 μ L base solution (25mM NaOH, 2mM EDTA). Base solutions from the isolates were
531 transferred to a PCR plate, boiled at 100°C for 20 min, and cooled at 4°C for 5 min.
532 20 μ L Tris solution (40mM Tris-HCl, pH 7.5) was then added to each sample. 1 μ L of this
533 sample was used as the DNA template for genotyping reactions. To identify which
534 isolates were the result of outcrossed mating, isolates were genotyped at two unlinked
535 microsatellite markers that are polymorphic between the R+ and R-parental strain (Levin
536 et al., 2014). All outcrossed diploids isolated were phenotypically thecate as opposed to
537 motile planktonic. No thecate isolates were observed in control EPCM treated cultures.

538 Isolation of haploid meiotic progeny: Immediately after phenotyping, clones isolated by
539 limiting dilution were passaged 1:10 into 1mL fresh 25% CG media to induce meiosis.
540 Thecate clones that were outcrossed diploids typically gave rise to a clear mixture of
541 haploid chains and rosettes after two days. Haploids were clonally isolated by limiting
542 dilution into 96-well plates containing 25% CG media, and phenotyped after five days.
543 Meiosis was confirmed either by 1) genotyping at two unlinked microsatellite markers, or
544 2) by genotyping at 38 markers using KASP technology (LGC Genomics, Beverly, MA)
545 (Levin et al., 2014).

546 Genotyping meiotic progeny: To confirm genome-wide recombination, haploid progeny
547 isolated from the 5% VFCM-induced cross were genotyped at 38 markers (Levin et al.,
548 2014). Briefly, three outcrossed diploids (named A2, A3, and H2) were rapidly passaged
549 to induce meiosis, and clones from each outcrossed diploid were isolated by limiting
550 dilution. The probability of clonal isolation at this step was .94 for A2, .93 for A3, and .91
551 for H2. A total of 147 haploid isolates from the three outcrossed diploids were
552 phenotyped and expanded for subsequent DNA extraction and genotyping.

553 **Quantifying mating swarms**

554 Inductions were set up in 100 μ L volumes in 96-well glass bottom plates (Ibidi
555 89626). Assays were imaged at 10X magnification using transmitted light (bright field)
556 on the Zeiss Observer Z.1 platform using a Hamamatsu C11440 camera. An automated
557 sequence was set up such that each sample was imaged at 4 distinct locations
558 throughout the well.

559 Images were batch processed in ImageJ to ensure consistency. After applying
560 the ‘Smooth’ command to reduce background bacterial signal, the ‘Find Edges’
561 command was applied to further highlight the phase-bright choanoflagellate cells.
562 Images were then converted to black and white using the ‘Make Binary’ command,
563 followed by the “Close” command to fill in small holes.

564 Finally, images were analyzed using the ‘Analyze Particles’ command to
565 calculate the area of each cell or swarm (the white space in Figure 2A’,B’) within an
566 image.

567 **Isolating the *Vibrio fischeri* mating induction factor**

568 Preparation of >30kD-enriched VCM: Eight 1L cultures of *V. fischeri* ES114 were grown
569 shaking for in 100% SWC for 24 h at 25°C. Cultures were pelleted at 16,000 \times g, and
570 the supernatants were concentrated to 120 mL using a tangential flow filtration device
571 with a 30 kDa centramate filter (Pall #OS030T12). The supernatant was then further
572 clarified by pelleting 39,000 \times g.

573 Ammonium sulfate precipitation: >30kD-enriched VCM was treated with 1 M Tris-HCl
574 (pH 7.6) and fractionally precipitated with increasing (40%-75%) concentrations of

575 ammonium sulfate. Precipitates were resuspended in water, and tested in the swarming
576 bioassay.

577 Size exclusion chromatography: Active ammonium sulfate precipitation fractions were
578 combined and concentrated to 1 mL. 0.85 mL was injected on a HiPrepTM 16/60
579 SephacrylTM S-200 High Resolution column (GE Healthcare Life Sciences #17-1166-01)
580 using an AKTA Explorer FPLC instrument. Proteins were eluted with 30 mM Tris-HCl
581 (pH 7.7, 4 °C) at 0.5 mL/min for 120 mL, and 2 mL fractions were collected. Adjacent
582 fractions were paired and tested in the swarming bioassay, as well as analyzed by
583 PAGE.

584 Anion exchange chromatography:

585 Active SEC fractions were combined and concentrated to 1 mL in Solvent A (20 mM L-
586 histidine, pH 6.0) and injected at 2.5 mL/min into a HiPrepTM 16/10 Q XL column (GE
587 Healthcare Life Sciences #17-5092-01). Proteins were eluted in 2 mL fractions over a
588 300 mL linear gradient (0-100%) of Solvent A to Solvent B (1 M NaCl in 20 mM L-
589 histidine, pH 6.0). Fractions were tested in the swarming bioassay and analyzed by
590 PAGE.

591 Renaturing proteins after PAGE: Proteins from highly active AEX fractions were
592 concentrated and mixed with 15 µg/mL β-lactoglobulin carrier protein, and run in
593 adjacent lanes through a NuPAGETM 4-12% Bis-Tris polyacrylamide gel. Evenly spaced
594 bands were excised from one lane, and the remaining gel was stained with Coomassie
595 blue R-250 and retained for mass spectrometry. The excised slices were crushed, and
596 then extracted for 6 hours with 300 µL of elution buffer (50 mM Tris-HCl pH 7.7, 100 µM
597 EDTA, 1 mM DDT, 150 mM NaCl, 0.1% sodium dodecyl sulfate [SDS], 100 µg/mL

598 bovine serum albumin [BSA], pH 7.7) (Hager and Burgess, 1980). Proteins were
599 precipitated with 1200 μ L cold acetone, incubated on dry ice for 30 minutes, and
600 pelleted at 16,000 \times g for 10 minutes at 4 °C. Air-dried pellets were dissolved in 10 μ L of
601 solubilization buffer (50 mM Tris-HCl pH 7.7, 100 μ M EDTA, 1 mM DDT, 150 mM NaCl,
602 20% glycerol, 6 M guanidine hydrochloride) for 20 minutes, and then diluted with 500 μ L
603 of dilution buffer (50 mM Tris-HCl pH 7.7, 100 μ M EDTA, 1 mM DDT, 150 mM NaCl,
604 20% glycerol). Proteins further renatured for 3.5 H at room temperature, and were
605 concentrated to 20 μ L. Proteins excised from bands were then tested in the swarming
606 bioassay.

607 **Mass Spectrometry:** Because only one excised protein band displayed bioactivity, the
608 corresponding slice retained for mass spectrometry was subjected to trypsin digestion
609 and LC-MS/MS at the Proteomics/Mass Spectrometry Laboratory at UC Berkeley.
610 Complete mass spectrometry results are listed in Supplemental File 2.

611 **Protein expression and purification**

612 The *eroS* gene was amplified by PCR (Phusion® DNA polymerase, New England
613 Biosciences) from *V. fischeri* ES114 genomic DNA (Forward primer: 5'-
614 GCCTCTGTCGACGCAAAAAATACCCAAACACCAC; Reverse primer: 5'-
615 AATTAAGCGGCCGCGTCTTGAATTGTTACTTGGAAAGAATAAG). After digestion
616 with *Sall*-HF and *Notl*-HF (New England Biolabs), the *eroS* gene was ligated in-frame
617 into a pET6xHN-N vector (Clontech) for fusion to a His-tag and transformed into
618 OneShot BL21(DE3) cells (Invitrogen) for expression. Transformed *E. coli* were grown
619 at 37 °C, 200 rpm shaking in LB media supplemented with 100 μ g/mL ampicillin. After
620 growth to OD 1.0, the temperature was decreased to 16 °C, and protein expression was

621 induced by addition of 1 mM IPTG. After 24 hours, cells were pelleted and lysed with
622 xTractorTM buffer (Clontech), purified with HisTALONTM gravity columns (Clontech), and
623 the His-tag was released by enterokinase cleavage (Millipore enterokinase cleave
624 capture kit #69067).

625 A gBlock of the *eroS* gene sequence harboring H278A and Y287A mutations was
626 purchased from Integrated DNA Technologies and ligated into the pET15b vector
627 (Novagen) at *NdeI* and *BamHI* restriction sites. The mutant *eroS* gene was transformed
628 into OneShot BL21 Star (DE3) cells (Invitrogen) for expression. Transformed *E. coli*
629 were grown at 37 °C, 220 rpm shaking in LB media supplemented with 100 µg/mL
630 ampicillin. After growth to OD 0.8, the temperature was decreased to 16 °C, and protein
631 expression was induced by addition of 0.3 mM IPTG. After 24 hours, cells were lysed
632 and protein was purified with HisPur Cobalt Resin (Thermo Scientific).

633 **Amino acid sequence alignments**

634 Amino acid sequences from *V. fischeri* (VF_A0994, GenBank: AAW88064.1) and
635 characterized bacterial GAG lyases [*A. aurescens* (AC lyase, PDB: 1RWG_A), *S.*
636 *coelicolor* (AC lyase, PDB: 2WDA_A), *S. agalactiae* (hyaluronate lyase, PDB: 1LXM_A),
637 *F. heparinum* (AC lyase, PDB: 1CB8_A), and *P. vulgaris* (ABC chondroitinase,
638 GenBank: ALL74069.1)] were aligned using Clustal Omega multiple sequence
639 alignment (<http://www.ebi.ac.uk/Tools/msa/clustalo/>). Conserved amino acid residues
640 were highlighted using BoxShade (http://www.ch.embnet.org/software/BOX_form.html).

641 **EroS GAG lyase activity *in vitro***

642 The glycosaminoglycan cleavage activity of purified Eros was determined *in vitro*
643 as previously described (Wang et al., 2015). Briefly, GAG standards [hyaluronic acid

644 (Sigma #H5388), chondroitin sulfate (Sigma #C4384), dermatan sulfate (Sigma
645 #C3788), and heparin (Sigma #H3393)] were dissolved to a concentration of 1 mg/mL in
646 buffer solution (50 mM NaH₂PO₄/Na₂HPO₄, 0.5 M NaCl, pH 8.0). 1 mL of GAG standard
647 was added to 5 µL of enzyme solution. The assays were performed in quartz cuvettes
648 (1 cm pathlength) at 23 °C, and UV absorbance measurements (232 nm) were taken
649 directly on the reacting mixture.

650 **AQUA quantification of EroS**

651 Absolute Quantification (AQUA) peptide (Gerber et al., 2003) was used to
652 accurately quantify the concentration of purified EroS and EroS in *Vibrio fischeri*
653 conditioned media. Briefly, *V. fischeri* was grown for 8 H in 100% SWC media and 5%
654 SWC media. Purified EroS and concentrated *Vibrio fischeri* culture supernatants were
655 loaded onto a PAGE gel. The gel was stained with Coomassie blue R-250, and bands
656 containing VF_A0994 were excised and sent to the Taplin Mass Spectrometry facility
657 (Harvard Medical School) for further analysis. Synthetic AQUA peptide
658 (TQITDDTYQNFFD[KC13N15], Sigma-Aldrich) and trypsin were added to each excised
659 band, and LC-MS/MS was performed on the digested peptides using a Thermo
660 Scientific Orbitrap. The amount of EroS present in each gel slice was calculated by
661 comparing MS2 peak intensities of the native peptide with the internal AQUA synthetic
662 peptide standard.

663 ***S. rosetta* polysaccharide isolation and GAG disaccharide analysis**

664 6 x 500 mL cultures of SrEpac were grown in 5% SWC until mid-stationary phase,
665 and washed 3x to reduce bacterial load before being pelleted, flash frozen, and

666 lyophilized. 125 mg of lyophilized *S. rosetta* sample was sent to the Complex
667 Carbohydrate Research Center for GAG isolation, digestion, and SAX-HPLC.

668 Polysaccharides were isolated from the *S. rosetta* sample and digested with
669 either EroS or chondroitinase ABC (Sigma C3667) for chondroitin disaccharide analysis,
670 and heparinases I, II, and III (Dextra Laboratories) for heparan disaccharide analysis.

671 Briefly, a ratio of 10 μ L *S. rosetta* polysaccharides to 1uL of enzyme was incubated for
672 24 hours. Samples were heated to 100°C for 5 minutes to inactivate the enzyme, and
673 centrifuged at 14,000 rpm for 30 minutes prior to SAX-HPLC.

674 SAX-HPLC was carried out on an Agilent system using a 4.6x250 mm Waters
675 Spherisorb analytical column with 5 μ m particle size at 25°C. Detection was performed
676 by post-column derivatization. Briefly, the eluent from the column was combined with a
677 1:1 mixture of 0.25 M NaOH and 1% 2-cyanoacetamide pumped at a flow rate of 0.5
678 mL/min from a post-column reactor. The eluent was heated to 130°C in a 10m reaction
679 coil, then cooled in a 50-cm cooling coil and directed into a Shimadzu fluorescence
680 detector ($\lambda_{\text{ex}} = 346$ nm, $\lambda_{\text{em}} = 410$). Commercial standard disaccharides (Dextra
681 Laboratories) were used for identification of each disaccharide based on elution time, as
682 well as calibration.

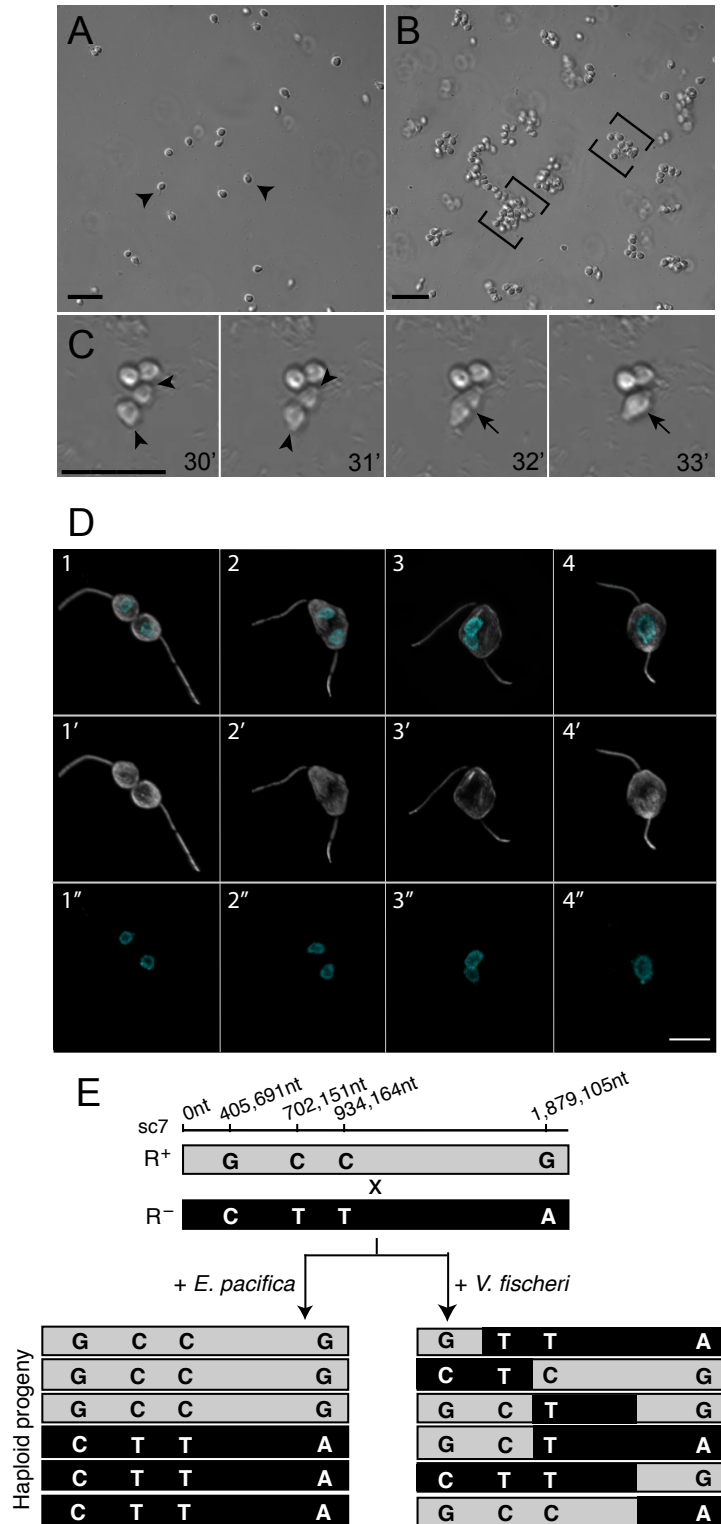
683 **Testing bioactivity of chondroitin disaccharides**

684 Chondroitin disaccharides and chondroitin sulfate were tested for bioactivity by
685 treating *S. rosetta* with unsulfated chondroitin disaccharides, chondroitin-6-sulfate
686 disaccharides, unsulfated chondroitin + chondroitin-6-sulfate disaccharides, and
687 chondroitin sulfate (from shark cartilage) at concentrations ranging from 0.0001M-0.1M.
688 Cells were imaged and quantified after 30 minutes, 1 hour, and 3 hours.

689 Degradation products of chondroitin sulfate were generated by incubating 100 µg
690 of chondroitin sulfate with 1µL of either EroS or ABC chondroitinase (*P. vulgaris*)
691 overnight. Enzymatic activity was killed by incubating samples at 80°C for 5 minutes.
692 The resulting degradation products were tested for bioactivity at concentrations ranging
693 from 0.0001M-0.1M. Cells were imaged and quantified after 30 minutes, 1 hour, and 3
694 hours.

695

696



697
698
699
700

Figure 1

701 **Figure 1. *V. fischeri* bacteria induce swarming and mating in the choanoflagellate,**
702 ***S. rosetta*.** **(A)** In the absence of *V. fischeri*, motile *S. rosetta* cells (arrowheads) are
703 evenly dispersed. **(B)** Within 30 minutes of exposure to *V. fischeri*, *S. rosetta* motile
704 cells aggregate into large swarms (brackets). Scale bar = 20 μ m. **(C)** *S. rosetta* cells
705 within a swarm pair and fuse. Prior to fusion, cells reposition themselves such that their
706 basal membranes are adjacent and their apical flagella point away (31'; arrowheads
707 mark apical pole of unfused cells). Cell fusion takes only minutes, and occurs along the
708 basal membrane (32'; indicated by arrow), resulting in a single, elongated cell (33';
709 indicated by arrow). Scale bar = 20 μ m. **(D)** Stages of cell and nuclear fusion in *S.*
710 *rosetta* mating pairs. Haploid mating pairs are oriented with their basal poles (opposite
711 the flagellum) touching (D1), and cell fusion proceeds along the basal membrane,
712 resulting in a binucleated cell with two flagella (D2). Nuclei then congress towards the
713 midline (D3), where the nuclei undergo nuclear fusion, resulting in a diploid cell (D4).
714 Anti-tubulin antibody (D1'-4'; white) highlights the cell body and flagellum, and Hoechst
715 (D1"-4"; cyan) highlights the nucleus. Scale bar = 5 μ m **(E)** Evidence for meiotic
716 recombination in *S. rosetta* following exposure to *V. fischeri*. Two haploid, genotypically
717 distinct *S. rosetta* strains [R+(grey shading) and R- (black shading)] were mixed in the
718 presence of either *E. pacifica* conditioned media (EPCM) or *V. fischeri* conditioned
719 media (VFCM) for 16 hours. Haploid progeny were clonally isolated and genotyped at
720 polymorphic markers across the genome (Supplemental Data). We show here
721 genotyping results for four representative loci along supercontig 7 (sc7). All clones
722 isolated from EPCM-treated cultures contained unrecombined parental genotypes, while

723 haploid clones isolated from VFCM-treated cultures showed clear evidence of
724 recombination. Top numbers show marker genomic positions along sc7.

725

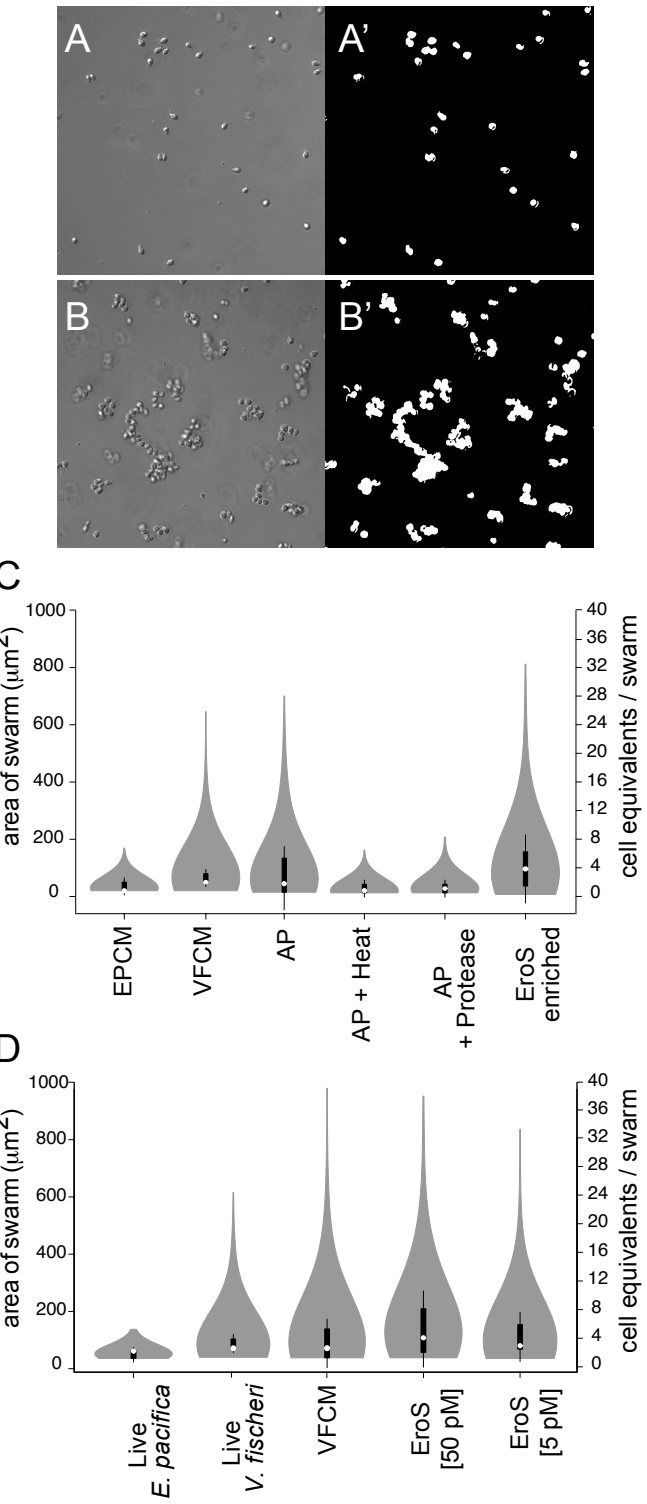


Figure 2

726
727

728 **Figure 2. Bioactivity-guided isolation of the *V. fischeri* aphrodisiac. (A, B)**

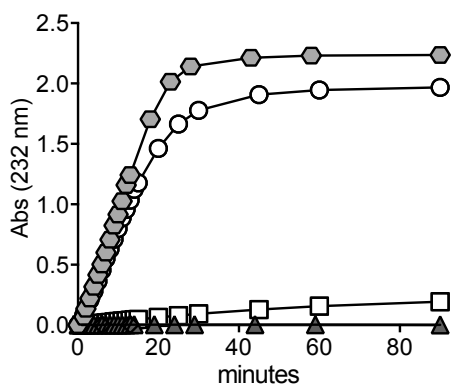
729 Automated image analysis allowed quantification of *S. rosetta* swarming in response to
730 *V. fischeri*-derived activity. Pictured are *S. rosetta* cells 30 minutes after treatment with
731 *E. pacifica* conditioned media (A) or *V. fischeri* conditioned media (B). By generating a
732 binary mask (A', B') we could measure the area of the swarm, and estimate the number
733 of cells (“cell equivalents”) per swarm. **(C)** Swarming in *S. rosetta* is induced by
734 compounds in the ammonium sulfate precipitation of *V. fischeri* culture supernatant (AP),
735 but not by AP exposed to heat (80°C for 10 minutes; AP + Heat) or proteases (AP +
736 Protease). The aphrodisiac activity tracked with a ~90kD protein band that was revealed
737 by mass spectrometry to be the *V. fischeri* EroS protein (VF_A0994). **(D)** EroS triggers
738 mating at plausible environmental concentrations. Purified EroS induces swarming in *S.*
739 *rosetta* at concentrations as low as 5 pM, and is sufficient to fully recapitulate the
740 aphrodisiac activity of live *V. fischeri* bacteria and VFCM.

741

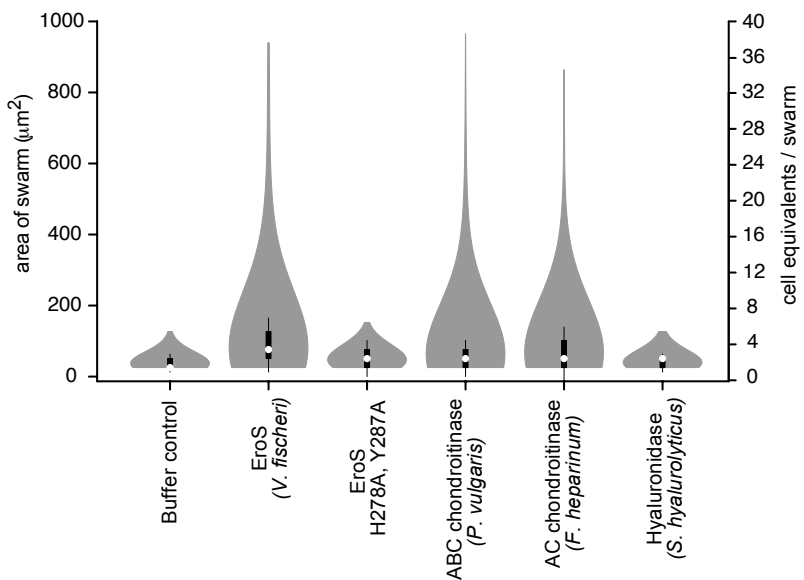
A

<i>V. fischeri</i>	SQATAALPAVIEYV--SEGDCYYTDGSFLQHSDIAYNGTYGNVLLGGI*GIQNAVAGSPWSMDNQT*SNV	317
<i>A. aurescens</i>	NHAVAGLSQVNQYV--TSGDGLERDGDFIQHSTTPYIGSYGVVLLIGLSKLFSLLGCTAEVSDPTRSIF	272
<i>F. heparinum</i>	SFAVKELFYPVQEYV--HYEIGIQLQYDSSYILOHGPOLQIISYCAVFIITGVIKLANYVRDTPYALSTEKIAIF	242
<i>S. coelicolor</i>	AIARDALSPVFFYV--TKGDGLYADGSFVQHTWVAYSGTYGQVMLDGLIGRLFTLLAGSEWEVTDPGRQLV	283
<i>S. agalactiae</i>	EKTSHSILKNIFTTA--TKAECYADGSYIDHTNVAYTCAAGNVLIDGLTQLLPIIQLFTDYKISNQEDDMV	606
<i>P. vulgaris</i>	NTFSHYITGALTQVPPGGKDGIRPDGIAWRHEGN-YPG-YSFPAFKNASQLIYLRLDTPESVGE SGWNNL	538

B



C



744 **Figure 3. The *V. fischeri* aphrodisiac is a chondroitinase. (A)** Alignment of the *V.*
745 *fischeri* EroS amino acid sequence to diverse bacterial GAG lyases reveals that *V.*
746 *fischeri* harbors conserved His and Tyr residues (indicated by *) at sites required for
747 catalytic activity in characterized GAG lyases. Amino acids with >50% conservation
748 between sequences are shaded (black shading for identical amino acids and grey
749 shading for similar amino acids. **(B)** Purified EroS degrades chondroitin sulfate and
750 hyaluronan. EroS was incubated with purified chondroitin sulfate (open circle),
751 hyaluronan (grey hexagon), dermatan sulfate (open square), and heparan sulfate (grey
752 triangle), and lyase activity of EroS was measured by monitoring the abundance of
753 unsaturated oligosaccharide products with an absorbance at 232nm. Chondroitin sulfate
754 and hyaluronan oligosaccharides accumulated rapidly in the presence of EroS,
755 indicating depolymerization, whereas heparan sulfate and dermatan sulfate were not
756 depolymerized by EroS. **(C)** The chondroitinase activity of EroS is necessary and
757 sufficient for its function as an aphrodisiac. EroS protein with mutations in predicted
758 catalytic resides (H278A, Y287A) fail to induce swarming in *S. rosetta*. *P. vulgaris* ABC
759 chondroitinase and *F. heparinum* AC chondroitinase are sufficient to induce swarming
760 at levels similar to EroS, whereas *S. hyalurolyticus* hyaluronidase fails to induce
761 swarming, indicating that chondroitinase activity is necessary and sufficient for
762 aphrodisiac activity.

763

764

765

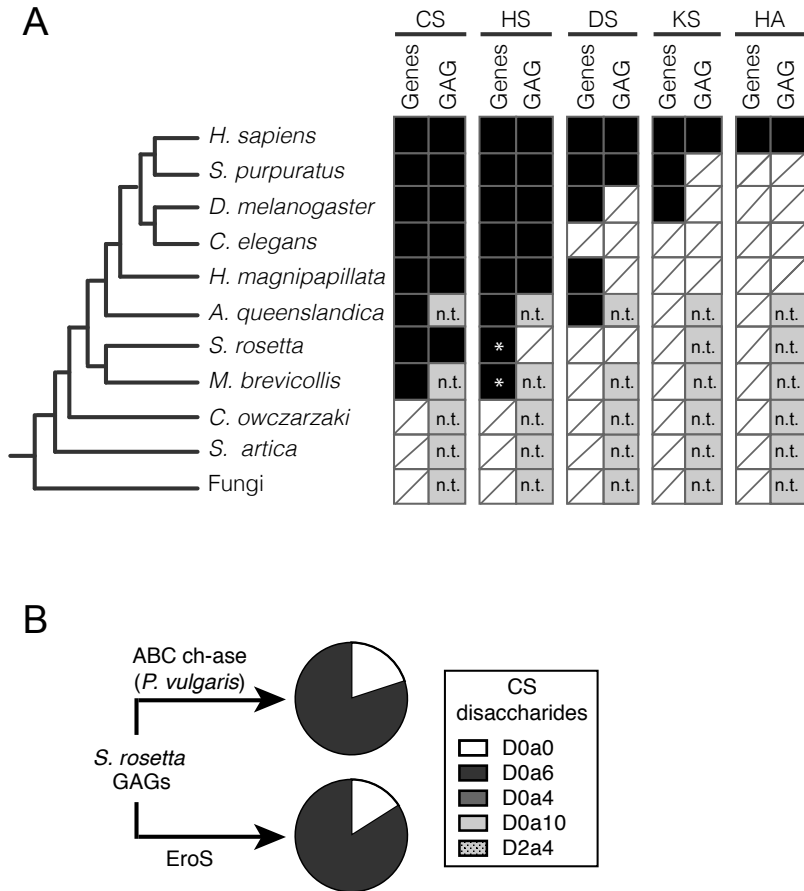


Figure 4

768 **Figure 4. *S. rosetta* produces chondroitin sulfate that can be degraded by EroS.**

769 **(A)** Phylogenetic distribution of diverse GAGs [CS= chondroitin sulfate; HS= heparan
770 sulfate; DS= dermatan sulfate; KS= keratan sulfate; HA= hyaluronan], and their
771 biosynthetic genes. The presence (black box) and absence (white box with slash) of
772 genes required for the biosynthesis of GAGs (Gene) and biochemical evidence for
773 GAGs (Expt) in select opisthokonts. *; Ori et al. (2011) identified putative homologs of a
774 subset of HS biosynthetic enzymes in the *M. brevicollis* genome, and we detect
775 homologs of the same limited set of HS biosynthetic enzymes in *S. rosetta*. Importantly,
776 these enzymes are shared components of the chondroitin biosynthetic pathway, and
777 digestion of *S. rosetta* polysaccharides with heparinases failed to liberate heparan
778 sulfate disaccharides, suggesting *S. rosetta* does not produce heparan sulfate (also
779 refer to Figure S3). n.t.; not tested (experiments have not been performed to
780 biochemically profile GAGs). **(B)** *S. rosetta* produces chondroitin that can be degraded
781 by EroS. Polysaccharides isolated from *S. rosetta* were treated with either *P. vulgaris*
782 ABC chondroitinase, an enzyme that can degrade many modifications of chondroitin
783 into its disaccharide units (CS disaccharides), or purified EroS. Both ABC
784 chondroitinase and EroS yielded similar amounts of unsulfated chondroitin
785 disaccharide (D0a0) and chondroitin-6-sulfate disaccharide (D0a6) degradation
786 products, indicating that unsulfated chondroitin and chondroitin-6-sulfate are produced
787 by *S. rosetta*. In contrast, we were unable to detect chondroitin-4-sulfate (D0a4),
788 chondroitin-4,6-sulfate (D0a10), or chondroitin-2,4-sulfate (D2a4) following degradation
789 of *S. rosetta* polysaccharides with either EroS or ABC chondroitinase.

Supplemental Information

An aphrodisiac produced by *Vibrio fischeri* stimulates mating in the closest living relatives of animals

Arielle Woznica^{a,1}, Joseph P Gerdt^{b,1}, Ryan E. Hulett^a, Jon Clardy^{b,2}, and Nicole King^{a,2}

^a Howard Hughes Medical Institute and Department of Molecular and Cell Biology, University of California, Berkeley, California 94720, United States

^b Department of Biological Chemistry and Molecular Pharmacology, Harvard Medical School, 240 Longwood Avenue, Boston MA 02115, United States

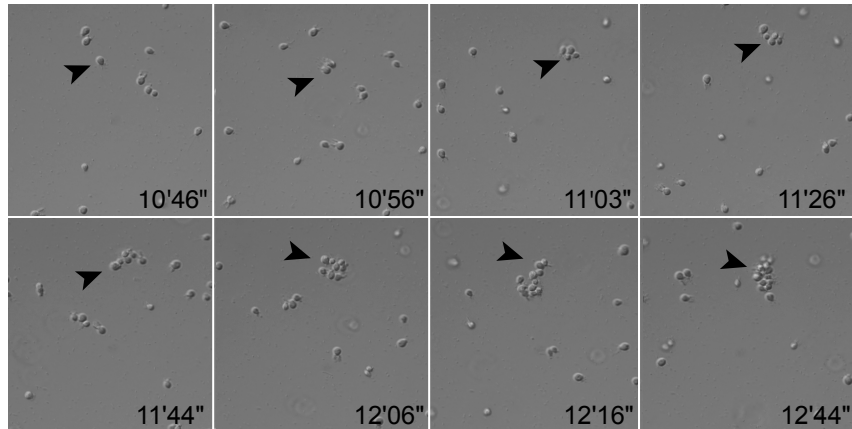
¹ These authors contributed equally to this work.

² Co-corresponding authors, jon_clardy@hms.harvard.edu and nking@berkeley.edu.

SI Table of Contents

SI Figures.....	3
SI File Descriptions.....	13
Supplemental Notes.....	14
Supplemental Tables.....	15

A



B

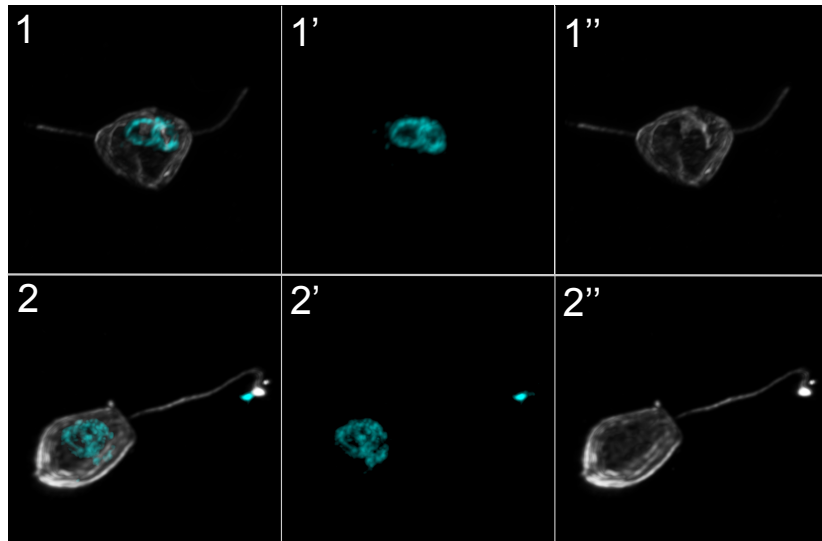


Figure S1

Figure S1 (related to Figure 1). *V. fischeri* induces swarming and mating in *S. rosetta*. **(A)** Stills of swarm formation after induction with *V. fischeri* bacteria. Arrowhead tracks the formation and movement of a single swarm over time. **(B)** Nuclear fusion in mating pairs of *S. rosetta* following treatment with *V. fischeri*. Pictured are late stages of nuclear congression and fusion. Following cell fusion, the nuclei congress towards the center of the bi-flagellated cell (B1-1’’), and fuse (B2-2’’). The final result of nuclear fusion is a diploid cell, harboring a single flagellum (B2-2’’). Hoechst (B1’,2’; cyan) highlights the nucleus, and anti-tubulin antibody (B1’’,2’’; white) highlights the cell body and flagellum.

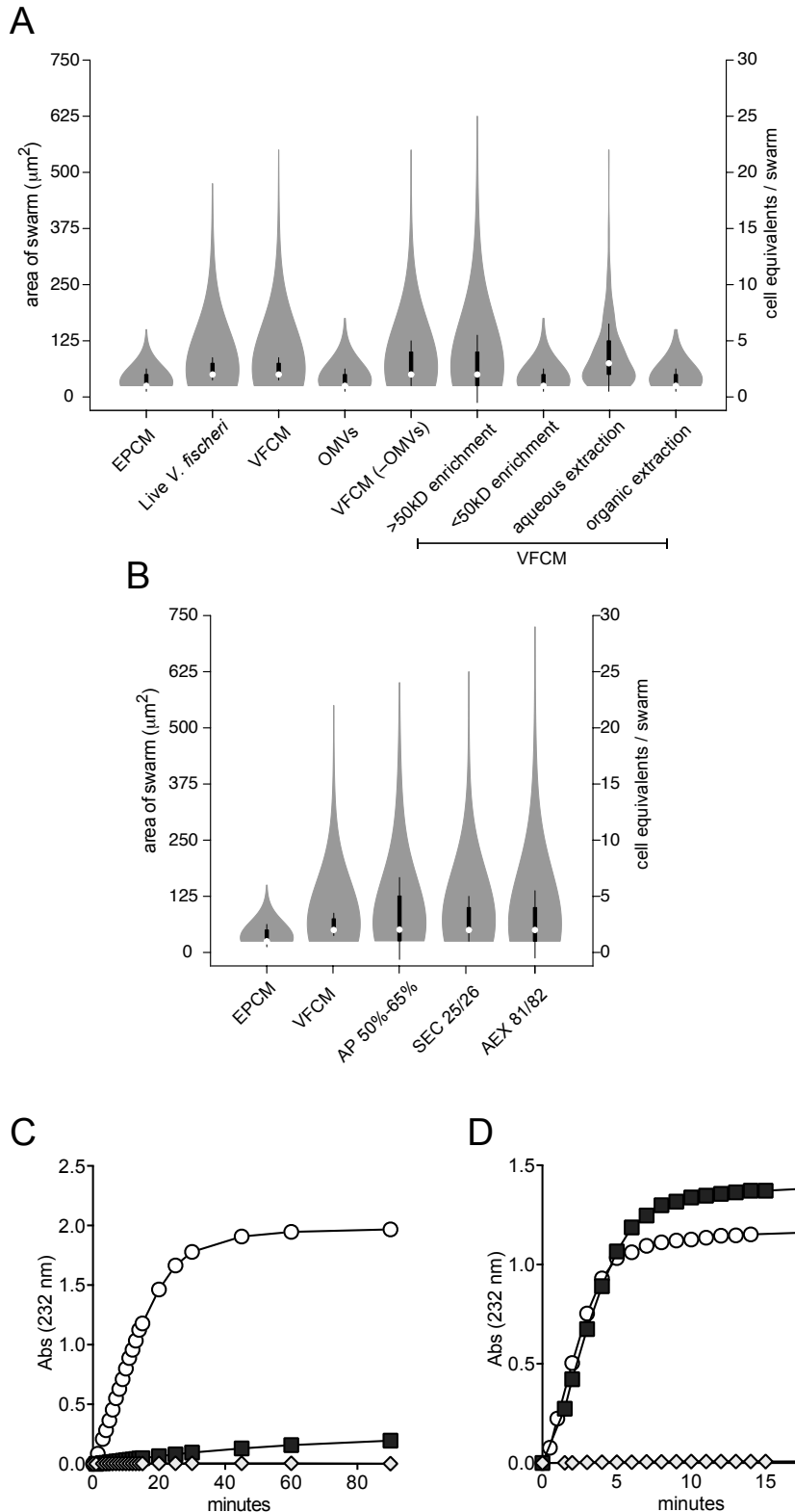


Figure S2

Figure S2 (related to Figure 2, Figure 3). Bioactivity-guided isolation and characterization of EroS. **(A)** Swarming in *S. rosetta* is induced by large (>50kD), water-soluble factors present in *V. fischeri* conditioned media (VFCM). **(B)** Isolation of EroS from VFCM. To identify the source of the aphrodisiac activity, proteins were precipitated from VFCM (AP 50%-65%) and separated by size exclusion (SEC) and anion exchange (AEX) chromatography. A protein band of ~90kD, later determined to be EroS (VF_A0994), was abundant in the bioactive SEC (SEC 25/26) and AEX (AEX 81/82) fractions. **(C, D)** EroS is a chondroitin AC lyase. **(C)** EroS degrades chondroitin sulfate AC, but not chondroitin sulfate B (dermatan sulfate) *in vitro*. EroS was incubated with purified chondroitin sulfate AC (open circle) and chondroitin sulfate B (dark grey square), and lyase activity of EroS was measured by monitoring the abundance of unsaturated oligosaccharide products with an absorbance at 232nm. Diamond represents a no enzyme control. **(B)** Chondroitinase ABC (*P. vulgaris*), a positive control for *in vitro* chondroitin degradation assays, rapidly depolymerizes both chondroitin sulfate AC (open circle) as well as chondroitin sulfate B (grey square). Diamond represents a no enzyme control.

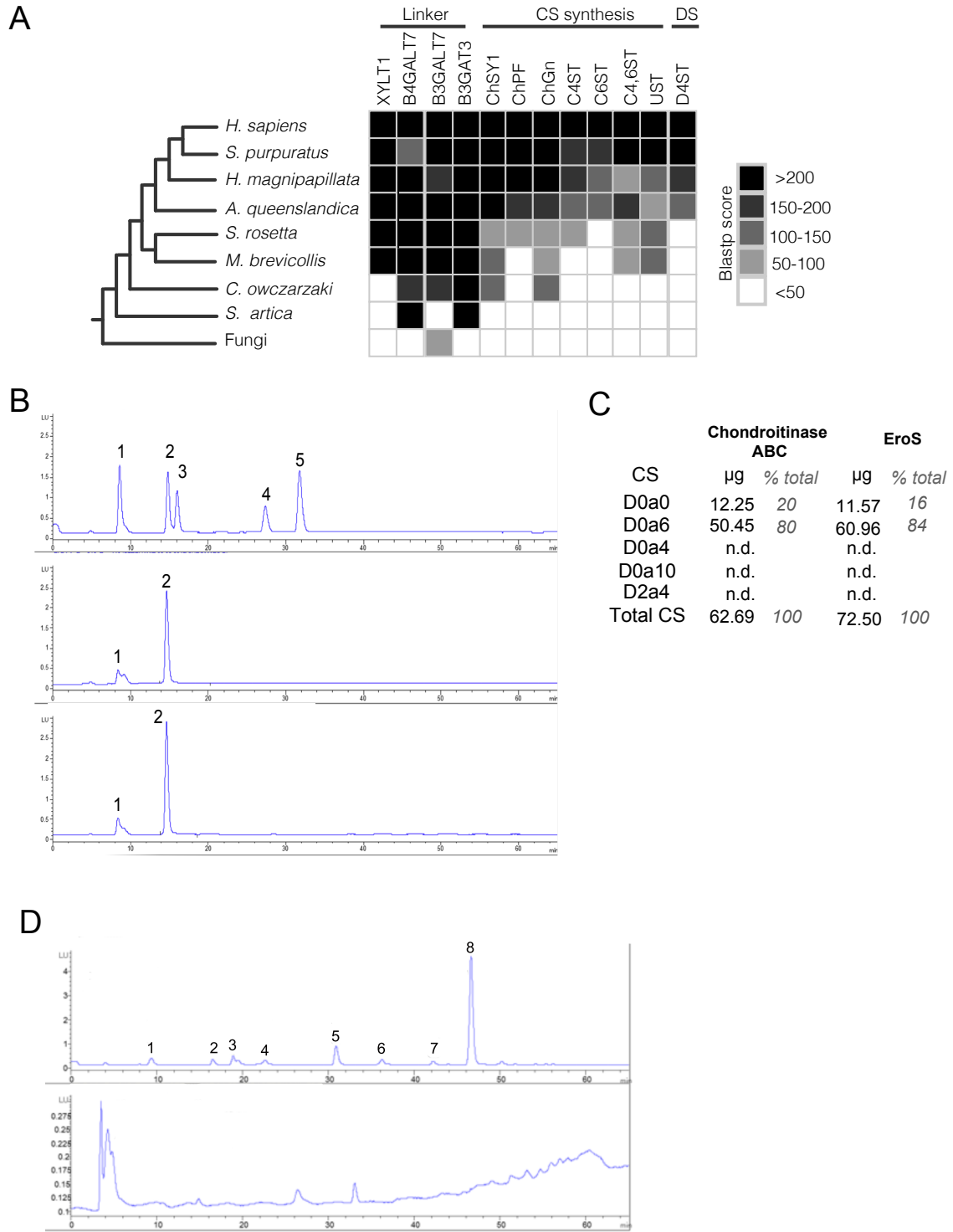


Figure S3

Figure S3. Chondroitin sulfate produced by *S. rosetta* can be degraded by EroS.

(A) Orthologs of chondroitin sulfate (CS) synthesis, but not dermatan sulfate (DS) synthesis, are present in the genomes of choanoflagellates *S. rosetta* and *M. brevicollis*. Genes identified as “linker” synthesize the proteoglycan linker tetrasaccharide and are important for the biosynthesis of multiple types of GAG, whereas the genes identified as “CS synthesis” are specific to CS biosynthesis. The gene identified as “DS” is required for the formation of dermatan sulfate. All query sequences used were human orthologs. If multiple subject sequences were hits for a single query sequence, the ortholog with the highest Blastp score was chosen. Query and subject accession information is provided in Supplemental File 3. **(B)** *S. rosetta* produces chondroitin that can be degraded by ABC chondroitinase and EroS. Polysaccharides isolated from *S. rosetta* were treated with either ABC chondroitinase from *P. vulgaris* (center plot) or EroS (bottom plot). Degradation products from samples treated with ABC chondroitinase and EroS were separated by SAX-HPLC (X-axis indicates time, Y-axis indicates abundance) and compared to the following chondroitin disaccharide standards (top plot): (1) D0a0, unsulfated chondroitin; (2) D0a6, chondroitin-6-sulfate; (3) D0a4, chondroitin-4-sulfate; (4) D0a10, chondroitin-4,6-sulfate; (5) D2a4, chondroitin-2,4-sulfate. Unsulfated and 6-sulfated chondroitin disaccharides were present at similar abundance in both the ABC chondroitinase and EroS –treated samples, whereas all other chondroitin disaccharides were below the limit of detection. **(C)** Quantification of chondroitin disaccharide products produced by ABC chondroitinase (*P. vulgaris*) and EroS treatment of *S. rosetta* polysaccharides. Disaccharide abbreviations: D0a0=unsulfated chondroitin; D0a6=chondroitin-6-sulfate; D0a4= chondroitin-4-sulfate; D0a10=chondroitin-4,6-sulfate; D2a4=chondroitin-2,4-sulfate. **(D)** *S. rosetta* does not produce heparan sulfate. Polysaccharides isolated from *S. rosetta* (bottom plot) were treated with Heparinase I, Heparinase II, and Heparinase III (Dextra Laboratories) separated by SAX-HPLC (X-axis indicates time, Y-axis indicates abundance) and compared to the following heparan sulfate disaccharide standards (top plot): (1) D0A0; (2) D0S0; (3) D0A6; (4) D2A0; (5) D0S6; (6) D2S0; (7) D2A6; (8) D2S6. No heparan disaccharides were present above the limit of detection in the *S. rosetta* polysaccharide sample.

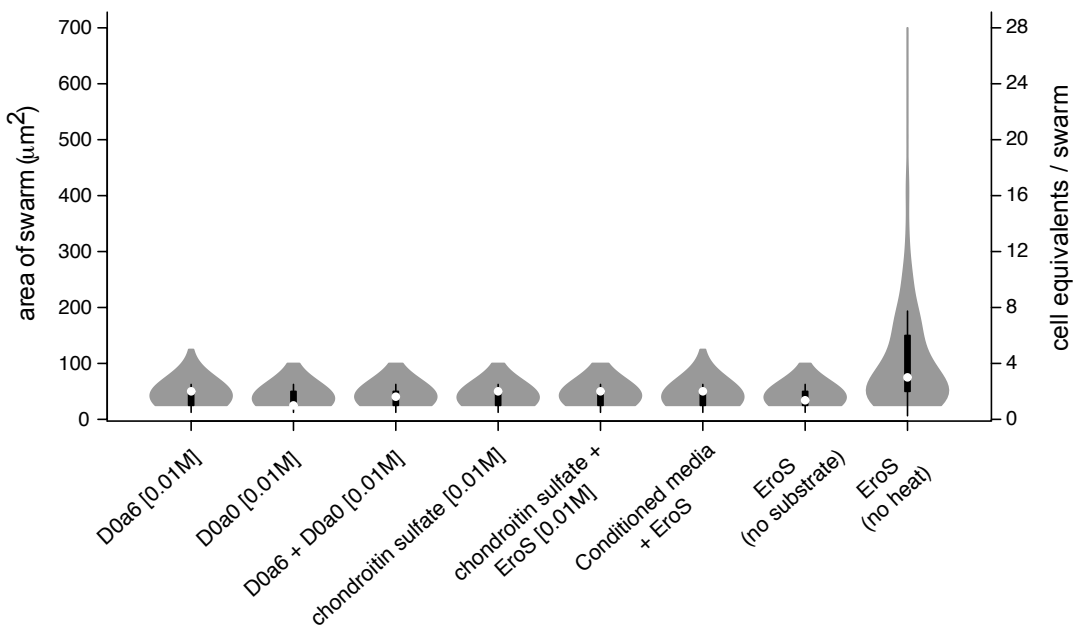


Figure S4

Figure S4. Swarming in *S. rosetta* is not induced by chondroitin sulfate or chondroitin disaccharides. Neither commercial chondroitin disaccharides (D0a6 and D0a0), chondroitin disaccharides generated via the depolymerization of chondroitin sulfate by EroS, nor conditioned media from EroS-treated *S. rosetta* cells are sufficient to induce swarming in *S. rosetta*.

A

<i>V. fischeri</i> density (cells/mL)	<i>S. rosetta</i> density (cells/mL)	# <i>Vibrio</i> : # <i>S. rosetta</i>	Time to swarm
2.0x10 ³	2.0x10 ⁶	1:1000	30 minutes
4.0x10 ²	2.0x10 ⁵	1:500	30 minutes
2.0x10 ²	2.0x10 ⁵	1:1000	60 minutes
4.0x10 ²	2.0x10 ⁴	1:50	30 minutes
1.0x10 ²	2.0x10 ⁴	1:200	90 minutes

B

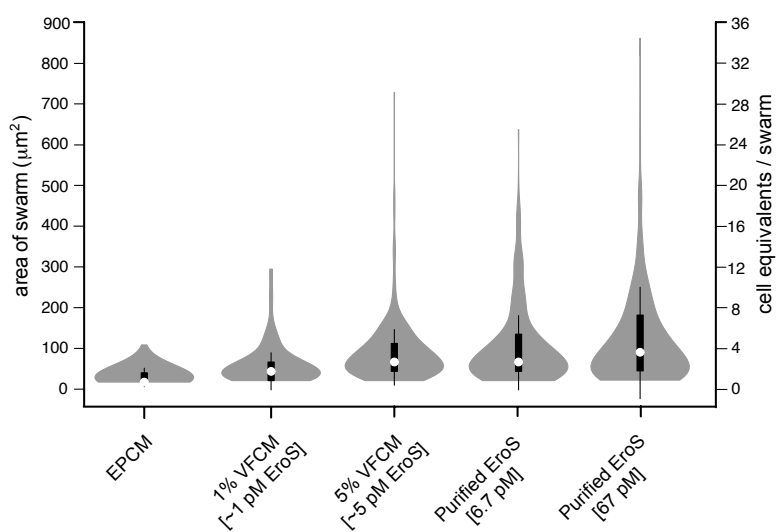


Figure S5

Figure S5. *V. fischeri* induces mating in *S. rosetta* under plausible environmental conditions (related to Table S4) . (A) *S. rosetta* swarms in response to low numbers of *V. fischeri* bacteria in a cell density-dependent manner. *S. rosetta* at high cell densities (2.0×10^6 cells/mL) swarms in response to as few as one *V. fischeri* cell per 1000 *S. rosetta* cells within 30 minutes of exposure, whereas swarming in *S. rosetta* at lower cell densities (2.0×10^5 cells/mL) within a similar time frame requires at least one *V. fischeri* cell per 500 *S. rosetta* cells. (B) Picomolar concentrations of secreted (5% VFCM) and purified EroS are sufficient to induce swarming in *S. rosetta*.

Movie S1 (related to Figure 1). Time-lapse movie of *S. rosetta* cells swarming in response to *V. fischeri*. The movie begins with a side-by-side comparison of *S. rosetta* treated with EPCM (left) and VFCM (right) one hour post induction.

After the short transition (“Induction with *V. fischeri*”) is a time-lapse depicting early swarm formation after treatment with 5% VFCM. All footage is displayed at 35x real time.

Movie S2 (related to Figure 1). Two cells within a four-cell swarm undergo cell fusion. Movie begins 30 minutes after addition of 5% VFCM. Cell fusion is displayed at 60X real time.

Supplemental File 1 (related to Figure 1). KASP genotyping of meiotic progeny isolated from *V. fischeri*- induced cross

Supplemental File 2 (related to Figure 2). Mass Spectrometry of bioactive *V. fischeri* protein fraction

Supplemental File 3 (related to Figure 3, Figure S3). Putative homologs of GAG biosynthetic enzymes

Supplemental Notes

Only 60 validated polymorphisms differentiate *S. rosetta* strains R+ and R- ²¹. Therefore, while we are able to detect independent assortment and recombination, because few markers sit within close proximity it was not possible to utilize genotyping data to accurately measure recombination frequency and construct linkage groups.

Supplemental Table 1. Bacteria tested in swarming bioassay (related to Figure 2)

Species	Strain	Genotype	Live bacteria	Conditioned media	Concentrated conditioned media	Accession information
<i>Vibrio fischeri</i>	ES114	WT			+	ATCC 700601
		ΔLuxO	+	+	+	Lupp et al. 2003
		ΔAinS	+	+	+	Lupp et al. 2003
		ΔLuxI	+	+	+	Lupp et al. 2003
		ΔAinSΔLuxS	+	+	+	Lupp and Ruby 2005
		ΔLuxR	+	+	+	Lupp and Ruby 2005
		ΔSypC	+	+	+	Shibata et al. 2012
		ΔSypH	+	+	+	Shibata et al. 2012
		ΔSypI	+	+	+	Shibata et al. 2012
		ΔSypK	+	+	+	Shibata et al. 2012
		ΔSypM	+	+	+	Shibata et al. 2012
		ΔSypO	+	+	+	Shibata et al. 2012
		ΔSypQ	+	+	+	Shibata et al. 2012
			+	+		Shibata et al. 2012
<i>Vibrio fischeri</i>	MJ11		+	+	+	BAA-1741
<i>Vibrio tubiashii</i>			+	+	+	ATCC 19105
<i>Vibrio orientalis</i>			+	+	+	ATCC 33934
<i>Vibrio harveyi</i>			-	-	-	ATCC 14126
<i>Vibrio natriegens</i>			-	-	-	ATCC 8110
<i>Vibrio parahaemolyticus</i>			Ψ	Ψ	Ψ	ATCC 17802
<i>Vibrio alginolyticus</i>			Ψ	Ψ	Ψ	PRJNA13571
<i>Vibrio anguillarum</i>			-	-	-	ATCC 19181
<i>Vibrio ordalii</i>			-	-	-	ATCC 33509
<i>Vibrio cholera</i>	YB1A01		n.t.	-	-	PRJNA281423
<i>Vibrio metoecus</i>	YB4D01		-	-	-	PRJNA281423
<i>Vibrio mimicus</i>			-	-	-	ATCC 33653
<i>Echinicola pacifica</i>			-	-	-	DSM 19836
<i>Echinicola pacifica</i>	From starved <i>S. rosetta</i> co-culture		n.t.	-	-	ATCC PRA-390

+: swarming observed; -: no swarming observed; Ψ: settling observed; n.t.: not tested

Supplemental Table 2. Purified molecules tested in swarming bioassay (related to Figure 2)

Molecule	Induces Swarming?	Source
3-O-C ₆ -(L)-HSL	–	Cayman Chemical (10011207)
C8-HSL	–	Cayman Chemical (10011199)
Cyclic di-GMP	–	Sigma SML1228
Chondroitinase ABC	+	Proteus vulgaris (Sigma C3667)
Chondroitinase AC	+	Flavobacterium heparinum (Sigma C2780)
Chondroitinase B	–	Flavobacterium heparinum (Sigma C8058)
Heparinase I and III	–	Flavobacterium heparinum (Sigma H3917)
Hyaluronate lyase	–	Staphylococcus hyalurolyticus (Sigma H113)
Chitinase	–	Streptomyces griseus (Sigma C9830)
O-Glycosidase	–	Streptococcus pneumonia (Sigma G1163)
Lysozyme	–	Sigma L67876
Collagenase	–	Clostridium histolyticum (Sigma C0130)
Unsulfated chondroitin	–	Sigma C3920
Chondroitin-6-sulfate	–	Sigma C4170
Chondroitin sulfate (shark cartilage)	–	Sigma C4384

Supplemental Table 3. Chondroitinase-induced mating in *S. rosetta* (related to Figure 3)

Inducing factor	Clonal isolates (#)	% thecate isolates (presumable diploid)	% outcrossed diploid isolates
<i>E. pacifica</i> CM (5% Vol/Vol)	88	0	0
EroS (<i>V. fischeri</i> , 50pM)	53	17%	15%
Chondroitinase ABC (<i>P. vulgaris</i> , 1 unit)	62	21%	17%
Chondroitinase AC (<i>F. heparinum</i> , 1 unit)	52	13%	11%

Supplemental Table 4. Quantification of purified EroS and EroS secreted by *V. fischeri* to Supplemental Figure 4)

	Purified EroS	Low nutrient media	High nutrient media
MS2 Peak intensity (sequence TQITDDTYQNFFDK)	1.43E+05	9.08E+02	2.77E+03
MS2 Peak intensity (1 pMol standard)	1.07E+04	2.24E+04	1.86E+04
pMol EroS in excised gel band	13.4	0.0405	0.149
Sample volume in gel band (μL)	2.0	18.0	6.0
[EroS] loaded on gel	6.7 μM	2.3 nM	25 nM
[EroS] in culture supernatant		6.8 pM	75 pM